Int. J. Morphol.,
43(2):385-393, 2025.

Histopathology and Immunoexpression of some Markers of Renal Fibrosis in the Hyperhomocysteinemic Sand Rat Model

Histopatología e Inmunoexpresión de algunos Marcadores de Fibrosis Renal en el Modelo Hiperhomocisteinémico de Rata de Arena

Billel Chaouad[1,2]; Elara N. Moudilou[3]; Adel Ghoul[1]; Fouzia Zerrouk[1]; Anissa Moulahoum[1]; Abdelhamid Sahraoui[2]; Jean-Marie Exbrayat[3] & Yasmina Benazzoug[1]

CHAOUAD, B.; MOUDILOU, E.N.; GHOUL, A.; ZERROUK, F.; MOULAHOUM, A.; SAHRAOUI, A.; EXBRAYAT, J.M. & BENAZZOUG, Y. Histopathology and immunoexpression of some markers of renal fibrosis in the hyperhomocysteinemic sand rat model. *Int. J. Morphol., 43(2)*:385-393, 2025.

SUMMARY: Several studies have shown that hyperhomocysteinemia (Hhcy), a risk factor for cardiovascular diseases, is also linked to other pathologies, including the aggravation of renal lesions in humans and some animal models. To our knowledge, no studies have been conducted on the potential impact of Hhcy on renal fibrosis and tissue remodeling in sand rats (*Psammomys obesus*). The aim of this study was to analyze renal histopathology as well as the immunoexpression of some fibrosis markers during Hhcy in sand rats. Hhcy was induced in this species by intraperitoneal administration of methionine (150 mg/kg body weight/day) for three months. The kidney removed at the end of the experiment was subjected to histomorphometric (Masson's trichrome staining, Sirius red) and immunohistochemical (collagen I and III, α-SMA, MMP-2 and -9) studies. Our results showed that the kidney of *Psammomys* Hhcy is the site of significant interstitial fibrosis, leukocytic infiltration, and disorganization of tubular and corpuscular structures. Immunohistochemistry revealed the involvement of type I and III fibrillar collagen in the development of fibrosis. Strong cytoplasmic immunoexpression of collagen I and III in inflammatory cells and α-SMA in the renal interstitium indicated the involvement of both leukocytes and myofibroblasts in the fibrosis process. Furthermore, we observed a decrease in MMP-2 and -9 immunoexpression in tubular cells and an increase in interstitial tissue and inflammatory cells. In conclusion, the kidneys of *Psammomys obesus* exhibited fibrosis and tissue remodeling secondary to Hhcy..

KEY WORDS: Hyperhomocysteinemia; Fibrosis; Kidney; *Psammomys obesus.*

INTRODUCTION

Hyperhomocysteinemia (Hhcy), a risk factor for cardiovascular diseases, is linked to other pathologies such as chronic kidney disease (CKD) development (Cohen *et al*., 2019). In patients with CKD, Hhcy is negatively correlated with glomerular filtration rate and positively associated with mortality risk (Shishehbor *et al*., 2008). The deleterious effects of Hhcy on the kidney are mediated by several mechanisms, including oxidative stress, inflammation, ER stress, DNA hypomethylation and fibrosis induction (Long & Nie, 2016). Renal fibrosis resulting from fibrillar collagens accumulation is a consequence of myofibroblast activation and proliferation (Huang *et al*., 2021). The localization of α-SMA, a marker of myofibroblasts, could be modified according to the nature and cause of renal pathology and probably to the animal model. Indeed, in rats with unilateral ureteral obstruction, α-SMA expression has been reported at the interstitial level, indicating a phenotypic change from fibroblasts to myofibroblasts (Li *et al*., 2020). In patients with glomerulonephritis, α-SMA is expressed at both interstitial and glomerular levels, showing phenotypic modulation of fibroblasts and mesangial cells (specialized pericytes) to myofibroblasts (Saratlija Novakovic *et al*., 2012). In diabetic mice, α-SMA expression is reported not at the interstitial level but in tubular epithelial cells, indicating Epithelial-Mesenchymal Transition (EMT) (Chen *et al*., 2016). Hhcy causes glomerulosclerosis in Sprague-Dawley rats, which is associated with a moderate increase in glomerular α-SMA

[1] Biochemistry and Remodelling of the Extracellular Matrix. Laboratory of Cellular and Molecular Biology. Faculty of Biological Sciences. University of Science and Technology Houari Boumediene (USTHB). Bab Ezzouar. Algiers, Algeria.
[2] University of Khemis Miliana. Faculty of Natural and Life Sciences and Earth Sciences, Khemis Miliana, Algeria.
[3] Sciences et Humanités (EA 1598), Lyon Catholic University (UCLy), Lyon, France.

Received: 2024-09-29 Accepted: 2024-12-11

expression, whereas at the interstitial level, no accumulation of collagens or α-SMA expression was observed (Cao *et al*., 2013). In contrast, the expression levels of metalloproteinases 2 and 9 (MMP-2 and -9) are upregulated during renal fibrosis (Cheng *et al*., 2017). Variations in MMP-2 and -9 expression in different renal structures and cells have been observed according to the origin of the renal pathology and its progressive stage (Cheng *et al*., 2017).

The sand rat (*Psammomys obesus*), a diurnal rodent in the Gerbillidae family, is considered a prime animal model for the study of type 2 diabetes, dyslipidaemia (Sahraoui *et al*., 2016), and Hhcy (Chaouad *et al*., 2019). Although several studies have examined some aspects of renal remodeling in diabetic sand rats (Aroune *et al*., 2017), the effect of Hhcy on this remodeling has not been investigated in this species. The aim of the study was to analyze the renal remodeling in hyperhomocysteinemic sand rats. We focused on possible variations in fibrillar collagen types I and III, α-SMA and metalloproteinase 2 and 9 localization, and their immunoexpression levels.

MATERIAL AND METHOD

Animal experiments. Our experiment, which lasted for 3 months, involved 10 male sand rats (*Psammomys obesus*). These animals were captured in the El-Outaya region, 20 km north of Biskra (East of Algeria) and placed in individual cages on arrival at the laboratory. After an adaptation period of 2 weeks in an animal house (temperature 25 °C, 50 % humidity, 12h light/dark cycle), the rats were divided equally into two groups:

- A control group (N=5) with a body weight of 131.36±12.72 g receives 50 g of halophilic plants daily.

- An experimental group (N=5) with body weight of 136.04±8.2 g received the same diet and intraperitoneal administration of 150 mg/kg body weight/day of DL-methionine (Sigma-Aldrich, 64340) dissolved in a 0.9 % NaCl solution.

At the end of the experiment, the animals were anesthetized by intraperitoneal injection of ketamine at 70 mg/kg body weight. Blood was then collected from the retro-orbital sinus of the eye using a heparinized Pasteur pipette to determine plasma homocysteine. After cervical dislocation and dissection, organs were removed and rapidly fixed in 10 % formalin for histological and immunohistochemical analyses. This study was approved by the Scientific Council of the faculty of biology at USTHB (N° 62/SDRFHU/2020). All experimental procedures were carried out in accordance with Algerian legislation (Law 12-235/2012 relating to the protection of animals), and the recommendations of the Algerian Association of Experimental Animal Sciences (N° 45/ DGLPAG/DVA/SDA/14).

Plasma homocysteine determination. Plasma homocysteine levels were measured using a fluorescence polarization enzyme immunoassay (FPIA). Indeed, all forms of homocysteine present in the plasma are reduced to free homocysteine by dithiothreitol. Total free homocysteine is transformed into S-adenosyl-l-homocysteine (SAH) by SAH hydrolase in the presence of excess adenosine. The sample containing only SAH was mixed with two reagents: one containing an anti-SAH monoclonal antibody, and the other containing a fluorescein-labeled S-adenosyl-L-cysteine tracer. SAH and the labeled tracer compete for the binding sites on the anti-SAH antibody. The intensity of fluorescence polarization was measured using the optical system of an analyzer (Abbott IMx).

Histological study. We used the common histological techniques to reveal the possible cellular and/or matrix alterations generated by Hhcy in *Psammomys obesus* kidneys. After fixation in 10 % formalin for two days, the organs were dehydrated in increasing alcohol bath (50 %, 70 %, 96 %, and 100 %) for 30 min each, and cleared in two butanol baths for 30 min each. After impregnation in molten paraffin (two baths of two hours each at 60 °C) and blocking, organs were cut using a Lab-Kite microtome. The 5µm thick sections were placed on Superfrost Plus slides and dried at 37 °C for 24 h. The slides were stained with Masson's Trichrome and Sirius red, which selectively stained the collagen fibers in red. Kidney histological sections were observed and analyzed using a Zeiss photonic microscope. Sections were photographed using a digital camera (Canon Power Shot A640) integrated with a Zeiss microscope.

Morphometric measurements and collagens quantification. Morphometric measurements were performed using CARL ZEISS AxioVision 4.9.1 software, following the calibration. For each parameter analysed at 1000 × magnification, 100 measurements were performed for each group of rats (on average, 20 randomly selected measurements per animal). The glomerular and corpuscular surfaces and their ratio were measured. In the proximal and distal convoluted tubules, cell height, tubular surface, luminal surface, and their ratio were assessed. Only transversely cut tubules were considered for these measurements.

Sirius red staining allowed us to quantify, in

percentage, fibrillar collagens in the intertubular interstitial space using the threshold function of image J software (1.47u-National Institutes of Health. USA). We randomly selected 10 tissue sections of the renal cortex devoid of renal corpuscles from each control and experimental animal (n = 5). The surface area of each section was 30,000 µm2 at 400 ¥ magnification.

Immunohistochemical analysis. Immunohistochemistry of collagen I and III, α-SMA, MMP-2 and -9 was performed using the Vectastain Elite Universal Kit (Vector Laboratories, CA, USA). Sand rat kidney histological sections were de-paraffinized in 2 cyclohexane baths for 15 min each and rehydrated in decreasing alcohol baths (100 %, 96 %, 70 %, and 50 %), followed by a distilled water bath. The sections were incubated for 40 min in 3 % H_2O_2 diluted in PBSx1 to block the endogenous peroxidase activity. After washing with PBSx1 and application of Dako-pen, the sections were incubated with 2 % BSA for 60 min to block non-specific antigenic sites. The primary antibody was applied to the sections at the following dilutions: 1/100 for rabbit polyclonal antibody anti-collagen I (Abcam ab34710), anti-collagen III (Abcam ab7778) and mouse monoclonal anti-a-SMA (Dako clone 1A4), 1/25 for rabbit polyclonal antibody anti-MMP-2 (Abcam ab37150) and anti-MMP-9 (Abcam ab38898). After application of the primary antibodies overnight at 4 °C, the sections were rinsed twice with PBSx1 for 5 min and incubated for 60 min with a biotinylated secondary antibody (Anti-Mouse/Anti-Rabbit IgG, Vector Laboratories, CA, USA). Another wash with PBSx1 was necessary before and after the 60 min application of the avidin-biotin-peroxidase complex. After revelation with Novared (peroxidase substrate, SK-4805, Vector Laboratories) and counterstaining with haematoxylin QS (Vector Laboratories, CA, USA), the sections were dehydrated and mounted in Permount. A negative control was used for each protein analyzed by omitting the primary antibody.

Immunohistochemical analysis was performed blindly by two qualified observers. They assigned the symbol (-) in the absence of staining in renal cells/compartments or one or more symbols (+) in the presence of staining, according to the degree of intensity and importance.

Statistical study. The results of the quantitative studies were analyzed using STATISTICA 6.1 software (StatSoft, Inc.). The mean and standard deviation were determined for each series of analyses. We used the Mann-Whitney U test to evaluate the differences between the quantitative parameters of the control and experimental animals. The difference was considered statistically significant if the P value was less than 0.05. This significant difference was represented as a percentage change in the experimental animals compared with the controls.

RESULTS

Homocysteinemia analysis. After 3 months of experimentation, we recorded a significant increase of about 884 % ($p<0.001$) in plasma Hcy in rats subjected to methionine compared with controls (20.86±1.75 vs 2.12±0.32 µM). Therefore, the methionine-treated group developed Hhcy.

Renal histomorphometry. In the kidneys of *Psammomys obesus*, Hhcy induced several histological alterations that affected both the nephron structure and surrounding interstitial tissue (Fig. 1). Indeed, we observed important infiltration of inflammatory cells at the interstitial level (Fig. 1. C), but also in the lumen of the renal tubules (Fig. 1. E). We also noticed disorganization of the proximal convoluted tubules, with heterogeneity in their tubular diameters (Fig. 1. F). Several distal convoluted tubules exhibited extensive luminal dilatation (Fig. 1. E). In addition, we observed an accumulation of collagens in the intertubular space and around the renal corpuscles, leading to renal fibrosis (Fig. 1. C, D, F).

Morphometric study (Table I) performed on some nephron parameters showed a significant change in all parameters analyzed in Hhcy rats compared to controls. Indeed, we recorded a significant increase of 38.53 % and 27.03 % in both corpuscular and glomerular surfaces, respectively. In contrast, the glomerular/corpuscular surface area ratio decreased by 10.78 %. In Hhcy rats, we noted inverse variations in morphometry between proximal and distal convoluted tubes. We noted in the proximal convoluted tubes a significant increase in epithelial cell height by 56.94 % and in the tubular surface by 51 %. In contrast, the luminal surface decreased by 39.94 % and the luminal/tubular surface ratio decreased by 59.39 %. In the distal convoluted tubules, there was a significant increase in epithelial cell height (27.27 %), tubular surface area (168.82 %), luminal surface area (471.76 %), and the luminal/tubular surface area ratio (109.3 %). Quantification of fibrillar collagens in the renal interstitium showed a significant increase of 116.33 % in Hhcy rats compared with control rats.

Immunohistochemical analysis. In the immuno histochemical study, we targeted the analysis of fibrillar collagen I and III to determine the type of collagen involved in renal fibrosis, α-SMA for the possible involvement of myofibroblasts, and MMP-2 and -9 to analyze the modulation of the biochemical composition of the renal extracellular matrix (ECM).

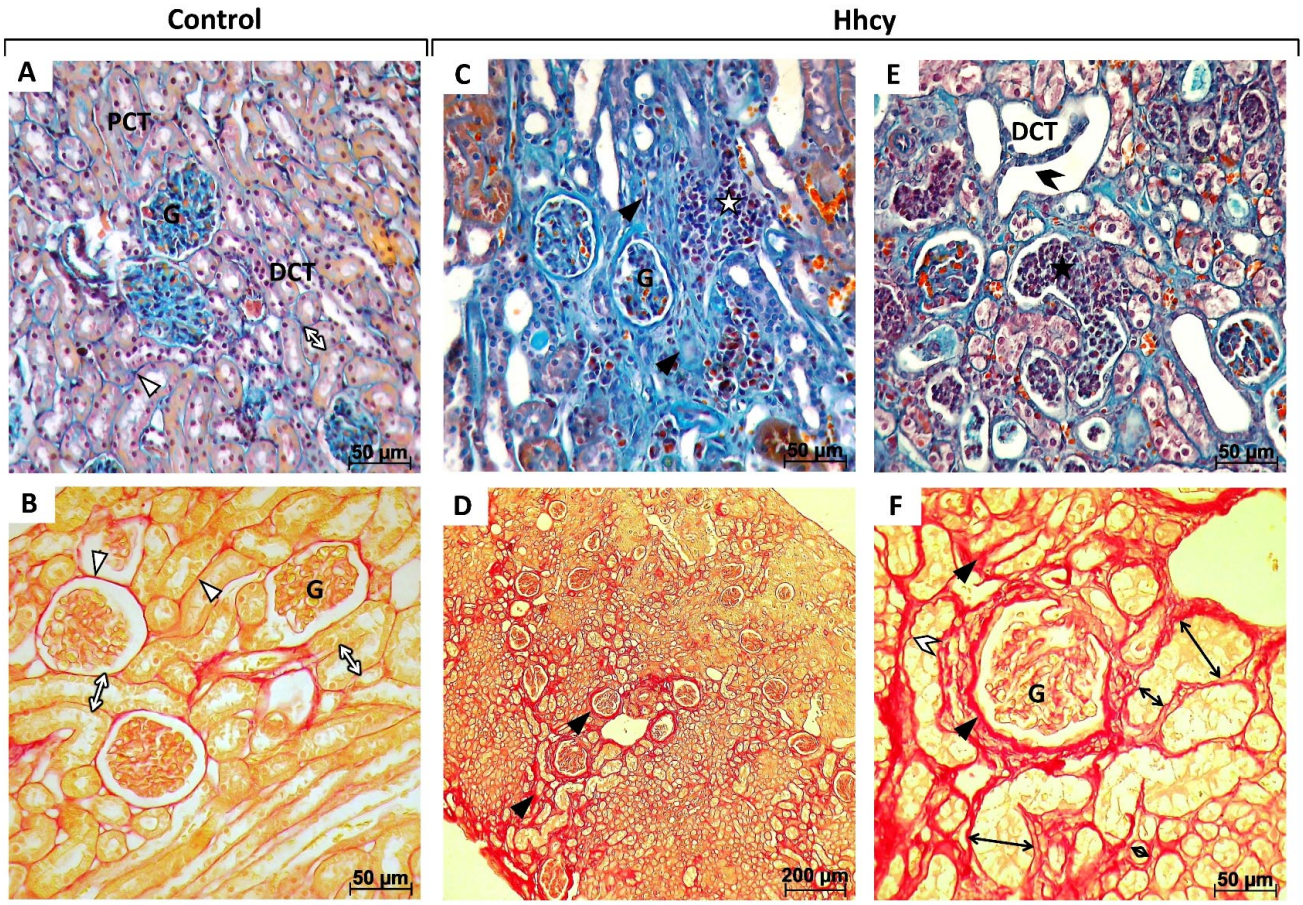

Fig. 1. Histology of the renal cortex of control (A, B) and Hhcy (C, D, E, F) *Psammomys obesus*. The top sections are stained with Masson's trichrome, and the bottom sections are stained with Sirius red. G: Glomeruli. PCT: Proximal Convoluted Tubule. DCT: Distal Convoluted Tubule. The renal cortex of control animals (A, B) showed a normal structure, where a weak presence of fibrillar collagen was observed between the tubules and around the renal corpuscles (white triangles). The proximal and distal convoluted tubules show a very homogeneous diameter (white arrows). In Hhcy rats (C, D, E, F), we observed an accumulation of collagen fibers in the renal interstitium and around the renal corpuscles (black triangles), heterogeneity in the diameter of the proximal convoluted tubules (black arrows), and disorganization of their structure (white chevron). Important leukocyt e infiltration is reported in the interstitial tissue (white star) and tubular lumen (black star). Many distal convoluted tubules showed luminal dilation (black chevron).

Table I. Morphometric study of some renal parameters and quantification of intertubular fibrillar collagen.

Parameters	Control	Hhcy	P-value
Renal corpuscles			
Corpuscular surface (µm²)	3702.49±136.85	5129.20±152.38	*P<0.0001*
Glomerular surface (µm²)	2700.77±91.84	3430.74±116.81	*P<0.0001*
Glomerular/corpuscular surface (%)	74.18 ± 0.78	66.22±0.63	*P<0.0001*
Proximal convoluted tubes			
Cell height (µm)	07.20±0.10	11.28±0.23	*P<0.0001*
Tubular surface (µm²)	622.82±15.21	940.43±21.65	*P<0.0001*
Luminal surface (µm²)	124.17±5.62	74.59±3.63	*P<0.0001*
Luminal/tubular surface (%)	19.68±0.62	7.99±0.36	*P<0.0001*
Distal convoluted tubules			
Cell height (µm)	04.40±0.08	05.55±0.15	*P<0.0001*
Tubular surface (µm²)	381.97±10.74	1026.91±37.28	*P<0.0001*
Luminal surface (µm²)	107.24±4.49	612.93±30.47	*P<0.0001*
Luminal/tubular surface (%)	27.74±0.71	57.88±1.13	*P<0.0001*
Fibrillar collagen/renal surface (%)	09.80 ± 0.44	21.2 ± 0.76	*P<0.0001*

Values are presented as mean ± SEM. A total of 100 measurements were performed for renal corpuscles and proximal and distal convoluted tubule parameters and 50 measurements for fibrillar collagen surface in control (n=5) and Hhcy (n=5) animals. Statistical test performed was the Mann-Whitney test.

In control rats, we observed a low accumulation of type I collagen in the tubulointerstitial tissue and around the renal corpuscles (Fig. 2. A). Type III collagen was very weakly expressed (Fig. 2. D). No labeling of collagen I or III was observed in the glomeruli. In Hhcy rats, we noticed significant accumulation of these two types of collagen in the interstitial tissue and around the renal corpuscles and blood vessels (Fig. 2. B, C, E, F). In contrast, very low deposition of collagen I and III was observed in the mesangial matrix of renal glomeruli. At the interstitial and perivascular levels, we observed strong granular immunostaining of collagen I and III in the cytoplasm of inflammatory cells (Fig. 2. B, C, E). This observation indicates that inflammatory cells are at least partially implicated in the synthesis of fibrillar collagens I and III.

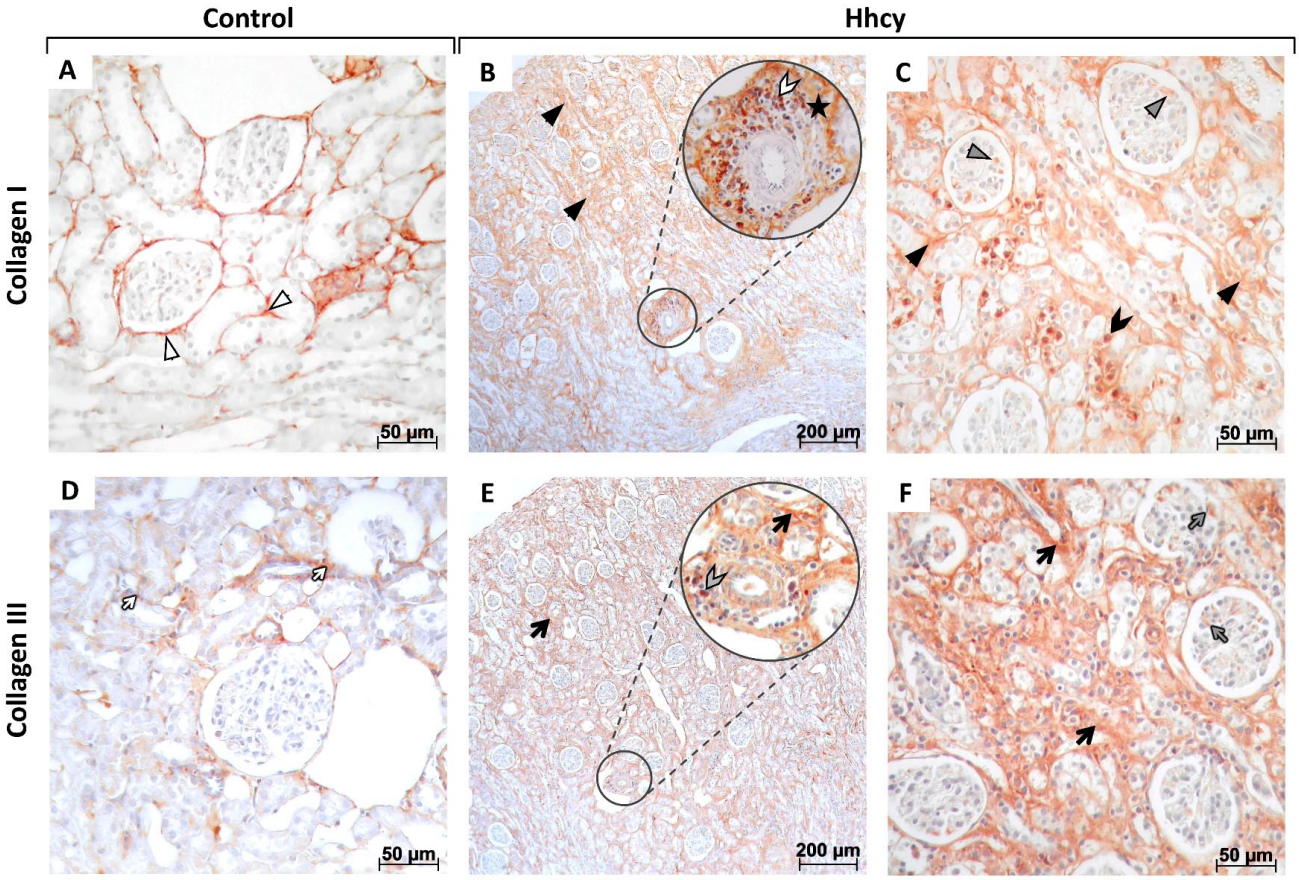

Fig. 2. Immunohistochemistry of fibrillar collagen I and III in the renal cortex of control and Hhcy *Psammomys* groups. In the control group (A), a low level of fibrillar collagen type I was observed between the tubules and around the renal corpuscles (white triangles). In Hhcy rats (B, C), we observed an important accumulation of collagen I between the tubules and around the renal corpuscles (black triangles), at the perivascular level (black star), and in the cytoplasm of inflammatory cells infiltrating the intertubular (black chevron) and perivascular spaces (white chevron). We also observed weak immunostaining for collagen I in the glomeruli of Hhcy rats (gray triangles). Concerning collagen III, we observed a very weak presence of this collagen type in the renal interstitial tissue (small white arrows) in the control group (D). In Hhcy group (E, F), we report an important accumulation of collagen III in the renal interstitium (large black arrows) with the appearance of weak immunostaining in the glomeruli (small gray arrows). Strong immunostaining for type III collagen was observed in perivascular inflammatory cells in Hhcy (gray chevron).

Immunostaining for α-SMA outside vascular smooth muscle cells (VSMCs) is an indication of myofibroblasts activation and proliferation, the major fibrillar collagen-producing cells. In control animals, we observed a few a-SMA-immunostained cells in the renal interstitial tissue (Fig. 3. A). In Hhcy rats, strong α-SMA immunostaining was observed in terms of intensity and extent in intertubular interstitial tissue (Fig. 3. B). No α-SMA immunostaining was observed in the glomeruli or tubular cells of the two animal groups.

Immunostaining analysis of MMP-2 and -9 indicates variability in their expression and localization between the kidneys of control and Hhcy *Psammomys.* In

the control rats, we observed strong immunoexpression of MMP-2 in the epithelial cell cytoplasm of the proximal and distal convoluted tubules (Fig. 3. C). A few rare cells express MMP-2 in the renal glomeruli, but no immunostaining has been reported in the tubulointerstitial tissue. In Hhcy rats, we observed weak immunostaining of MMP-2 in tubular cells and tubulointerstitial tissue, and very strong labeling in inflammatory cells (Fig. 3. D). The number of cells expressing MMP-2 in the glomeruli was higher in Hhcy rats than in the control rats. Regarding MMP-9, we observed weak immunostaining in tubular cells but no labeling in glomeruli or interstitial tissue (Fig. 3. E). In Hhcy rats, we observed strong immunostaining at the interstitial level and very strong labeling of the inflammatory cells (Fig. 3. F). No labeling was observed in the tubular and glomerular cells. All these observations are summarized in Table II.

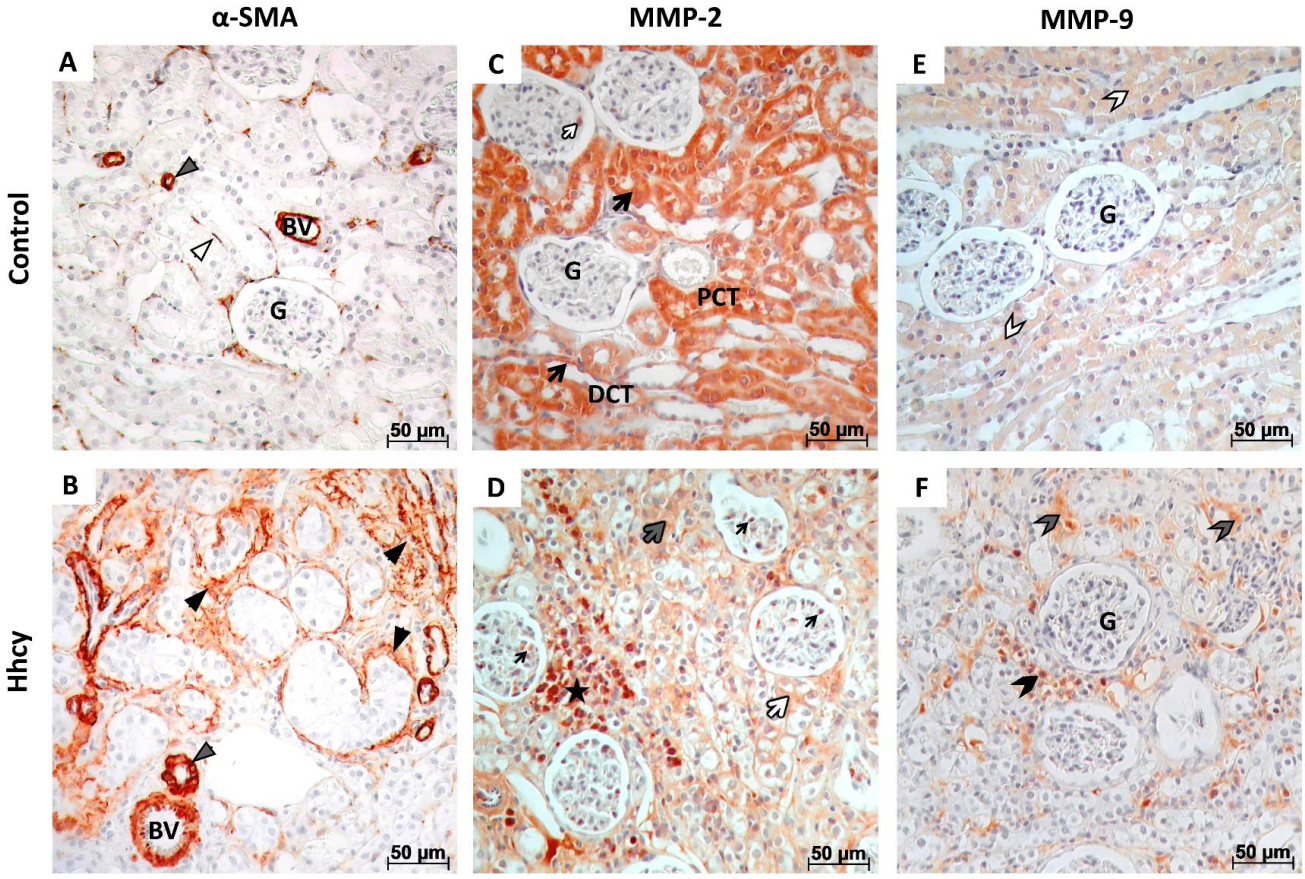

Fig. 3. Immunohistochemistry of a-SMA, MMP-2 and -9 in the renal cortex of control and Hhcy *Psammomys* groups. G: Glomeruli. PCT: Proximal Convoluted Tubule. DCT: Distal Convoluted Tubule. BV: Blood Vessel. Excluding the strong immunostaining of a-SMA in VSMCs of both groups of animals (gray triangles), we observed in control group (A) some myofibroblasts expressing a-SMA between the renal tubules (white triangle). In Hhcy group (B), strong immunoexpression of a-SMA (black triangles) was observed between the renal tubules. Strong immunostaining of MMP-2 was reported in control animals (C) in renal tubule cells (large black arrows) and some glomerular cells (small white arrow). In Hhcy rats (D), weak immunostaining of MMP-2 was observed in renal tubule cells (large gray arrow) and interstitial tissue (large white arrow), and strong immunostaining was observed in inflammatory cells (black star). The number of cells expressing MMP-2 increased in the glomeruli of Hhcy rats (small black arrows). Concerning MMP-9, very weak immunolabelling was observed in renal tubule cells (white chevrons) of control rats (E). In Hhcy rats (F), weak immunostaining was observed in the interstitial tissue (gray chevrons) and was slightly stronger in the inflammatory cells (black chevron).

DISCUSSION

The objective of this study was to analyze renal remodeling and fibrosis in sand rats with Hhcy using histomorphometric and immunohistochemical approaches. Our results show that Hhcy in *Psammomys* kidneys is the site of interstitial fibrosis and inflammatory cell infiltration. Hhcy increases endothelial cell adhesion and induces a pro-inflammatory state in the vascular wall by promoting the expression of adhesion molecules and recruitment of

Table II. Immunolocalization and immunostaining intensity of collagen I and III, α-SMA, MMP-2 and -9 in the kidney of control and Hhcy rats.

Immunolocalization	Control	Hhcy
Collagen I		
Glomeruli	-	+
Tubular cells	-	-
Interstitial tissue	++	+++++
VSMCs	-	-
Inflammatory cells	-	++++
Collagen III		
Glomeruli	-	+
Tubular cells	-	-
Interstitial tissue	+	+++++
VSMCs	-	-
Inflammatory cells	-	++++
α-SMA		
Glomeruli	-	-
Tubular cells	-	-
Interstitial tissue	+	++++
VSMCs	++++	++++
Inflammatory cells	-	-
MMP-2		
Glomeruli	+	++
Tubular cells	++++	++
Interstitial tissue	-	+++
VSMCs	-	-
Inflammatory cells	-	++++
MMP-9		
Glomeruli	-	+
Tubular cells	++	+
Interstitial tissue	-	++
VSMCs	-	-
Inflammatory cells	-	+++

Absence of immunohistochemical markers (-). Estimation of the importance of immunohistochemical marker by observation (+).

monocytes, particular MCP-1 (Monocyte chemoattractant protein-1), interleukin-8, VCAM-1 (Vascular cell adhesion molecule 1), ICAM-1 (Intercellular adhesion molecule) and endothelin-1 (Yuan *et al*., 2022). According to Zhang *et al*. (2004), Hhcy activates NF-kB and induces iNOS expression in the kidney, consequently increasing peroxynitrite formation. Peroxynitrite alters the redox state of the vascular wall, thereby increasing the expression of VCAM-1, ICAM-1, E-selectin, and MCP-1 in endothelial cells (Huang, 2003). In view of these data, it would probably be interesting to analyze some markers of inflammation, notably VCAM-1, ICAM-1 and MCP-1.

Interstitial fibrosis in the kidneys of Hhcy animals is a result of fibrillar collagen types I and III accumulation. According to Huang *et al*. (2021), renal fibrosis is a typical feature of CKD and represents the final common pathway in all progressive kidney diseases. Interstitial fibrosis has been reported in the kidneys of Fisher rats, rendering Hhcy by a diet supplemented with methionine (1.25 %) and deficient in folate for 12 weeks (Kumagai *et al*., 2002). Similarly, a diet low in methionine in mice decreased plasma homocysteine concentrations and reduced some markers of renal fibrosis and inflammation (Cooke *et al*., 2018). According to several recent studies, including those by Wang *et al*. (2022), type I and type III collagens are involved in interstitial and perivascular fibrosis during CKD in humans and in some animal models.

In Hhcy rats, we also noted strong collagen I and III labeling in inflammatory cells, indicating that these cells are involved in renal fibrosis. To find out whether myofibroblasts are similarly involved in fibrosis, we analyzed α-SMA. We reported in Hhcy rats a significant increase in interstitial a-SMA immunoexpression, indicating the proliferation and differentiation of fibroblasts into myofibroblasts. Numerous studies have demonstrated that myofibroblasts, which are reactive under pathological conditions, are responsible for the accumulation of interstitial ECM components, such as type I and III collagens (Kramann *et al*., 2013). Cao *et al*. (2013) observed glomerulosclerosis associated with increased glomerular a-SMA expression in Sprague Dawley rats. In contrast to our results, these investigators did not report interstitial fibrosis or α-SMA interstitial expression. Similarly, Ossani *et al*. (2004) reported no interstitial fibrosis or glomerulosclerosis in Wistar rats subjected to moderate Hhcy for 10 and 44 weeks. These authors noted no change in α-SMA expression between the Hhcy and control rats. Taken together, these results suggest that sand rats may be more sensitive to Hhcy in the development of interstitial fibrosis than laboratory rats.

Renal matrix remodeling involves variations in the expression of MMPs, particularly MMP-2 and -9 in patients with CDK (Cheng *et al*., 2017). From this perspective, we analyzed, by immunohistochemistry, the possible modifications of these remodeling factors in the kidney of Hhcy *Psammomys*. We reported a high expression of MMP-2 in proximal and distal tubular cells in the kidneys of control rats. MMP-9, on the other hand is very weakly expressed in these cells. These observations are in agreement with Cheng *et al*. (2017), who reported that, under physiological conditions, MMP-2 and -9 are found in the inactive zymogenic form (pro-MMPs) in renal tubular cells. Similarly, Nee *et al*. (2004) reported that in cultured human proximal tubule cells, no detectable MMP-9 production was observed, whereas the pro-MMP-2 form was visible. In tubular cells from our Hhcy rats, MMP-2 expression decreased, whereas MMP-9 expression became undetectable. MMP-2 and -9 appears in the tubulointerstitial tissue of Hhcy rats. These results suggest that MMP-2 and -9 are

constitutively synthesized in renal tubular cells of *Psammomys* in an inactive latent form. Hhcy causes the release of these metalloproteinases into the interstitial space and their activation. Tsai *et al*. (2012) found that renal fibrosis is associated with decreased expression of MMP-9 in the cytoplasm of normal tubular. Hhcy causes an increase in the expression of active and latent forms of MMP-2 and -9 in the renal cortex of CBS+/- mice (Sen *et al*., 2010). MMP-2 accelerates late-stage macrophage infiltration in a mouse model of unilateral ureteral obstruction, probably by degrading ECM components (Nishida *et al*., 2007).

Furthermore, we demonstrated renal tubular dilatation in Hhcy rats. According to Gaut & Liapis (2020), acute kidney injury is characterized by focal or diffuse tubular luminal dilatation in the proximal tubules. Kumagai *et al*. (2002) showed renal tubular dilation in Fisher rats rendered Hhcy by a folate-deficient diet for 12 weeks. According to the same study, combining this diet with methionine (1.25 %) increases the tubular dilation.

CONCLUSION

In summary, hyperhomocysteinemia induces cellular and extracellular matrix remodeling in the kidneys of *Psammomys obesus*, characterized by interstitial fibrosis, leukocytic infiltration, and nephrotic structure disorganization. Fibrosis, resulting from the accumulation of type I and III collagens, is associated with interstitial proliferation of myofibroblasts and alterations in the intensity and localization of MMP-2 and MMP-9 immunoexpression.

CHAOUAD, B.; MOUDILOU, E.N.; GHOUL, A.; ZERROUK, F.; MOULAHOUM, A.; SAHRAOUI, A.; EXBRAYAT, J-M. & BENAZZOUG, Y. Histopatología e nmunoexpresión de algunos marcadores de fibrosis renal en el modelo hiperhomocisteinémico de rata de arena *Int. J. Morphol., 43(2)*:385-393, 2025.

RESUMEN: Varios estudios han demostrado que la hiperhomocisteinemia (Hhcy) es un factor de riesgo para las enfermedades cardiovasculares, que también está relacionada con otras patologías, incluido el agravamiento de las lesiones renales en humanos y algunos modelos animales. Hasta donde sabemos, no se han realizado estudios sobre el posible impacto de la Hhcy en la fibrosis renal y la remodelación tisular en ratas de arena (*Psammomys obesus*). El objetivo de este estudio fue analizar la histopatología renal, así como la inmunoexpresión de algunos marcadores de fibrosis durante la Hhcy en ratas de arena. La Hhcy se indujo en esta especie mediante la administración intraperitoneal de metionina (150 mg/kg de peso corporal/día) durante tres meses. El riñón extirpado al final del experimento fue sometido a estudios histomorfométricos (tinción tricrómica de Masson, Rojo Sirio) e inmunohistoquímicos (colágeno I y III, α-SMA, MMP-2 y -9). Nuestros resultados mostraron que el riñón de *Psammomys* Hhcy es el sitio de fibrosis intersticial significativa, infiltración leucocítica y desorganización de las estructuras tubulares y corpusculares. La inmunohistoquímica reveló la intervención de colágeno fibrilar de tipo I y III en el desarrollo de la fibrosis. La fuerte inmunoexpresión citoplasmática de colágeno I y III en células inflamatorias y de α-SMA en el intersticio renal indicó la intervención tanto de leucocitos como de miofibroblastos en el proceso de fibrosis. Además, observamos una disminución de la inmunoexpresión de MMP-2 y -9 en células tubulares y un aumento en el tejido intersticial y en células inflamatorias. En conclusión, los riñones de *Psammomys obesus* mostraron fibrosis y remodelación tisular secundaria a la Hhcy.

PALABRAS CLAVE: Hiperhomocisteinemia; Fibrosis; Riñón; *Psammomys obesus*.

REFERENCES

Aroune, D.; Libdiri, F.; Leboucher, S.; Maouche, B.; Marco, S. & El-Aoufi, S. Changes in the NFkB and E-cadherin expression are associated to diabetic nephropathy in *Psammomys obesus*. *Saudi J. Biol. Sci., 24(4)*:843-50, 2017.

Cao, L.; Lou, X.; Zou, Z.; Mou, N.; Wu, W.; Huang, X. & Tan, H. Folic acid attenuates hyperhomocysteinemia-induced glomerular damage in rats. *Microvasc. Res., 89*:146-52, 2013.

Chaouad, B.; Moudilou, E.N.; Ghoul, A.; Zerrouk, F.; Moulahoum, A.; Othmani-Mecif, K.; Cherifi, M.E.H.; Exbrayat, J. M. & Benazzoug, Y. Hyperhomocysteinemia and myocardial remodeling in the sand rat, *Psammomys obesus*. *Acta Histochem., 121(7)*:823-32, 2019.

Chen, N.; Hao, J.; Li, L.; Li, F.; Liu, S. & Duan, H. Carboxy-terminal modulator protein attenuated extracellular matrix deposit by inhibiting phospho-Akt, TGF-b1 and a-SMA in kidneys of diabetic mice. *Biochem. Biophys. Res. Commun., 474(4)*:753-60, 2016.

Cheng, Z.; Limbu, M.; Wang, Z.; Liu, J.; Liu, L.; Zhang, X.; Chen, P. & Liu, B. MMP-2 and 9 in chronic kidney disease. *Int. J. Mol. Sci., 18(4)*:776, 2017.

Cohen, E.; Margalit, I.; Shochat, T.; Goldberg, E. & Krause, I. The relationship between the concentration of plasma homocysteine and chronic kidney disease: a cross sectional study of a large cohort. *J. Nephrol., 32(5)*:783-9, 2019.

Cooke, D.; Ouattara, A. & Ables, G. P. Dietary methionine restriction modulates renal response and attenuates kidney injury in mice. *FASEB J., 32(2)*:693-702, 2018.

Gaut, J. P. & Liapis, H. Acute kidney injury pathology and pathophysiology: a retrospective review. *Clin. Kidney J., 14(2)*:526-36, 2020.

Huang, A.; Guo, G.; Yu, Y. & Yao, L. The roles of collagen in chronic kidney disease and vascular calcification. *J. Mol. Med. (Berl.), 99(1)*:75-92, 2021.

Huang, P. L. Endothelial nitric oxide synthase and endothelial dysfunction. *Curr. Hypertens. Rep., 5(6)*:473-80, 2003.

Kramann, R.; DiRocco, D. P.; Maarouf, O. H. & Humphreys, B. D. Matrix-producing cells in chronic kidney disease: origin, regulation, and activation. *Curr. Pathobiol. Rep., 1(4)*:301-11, 2013.

Kumagai, H.; Katoh, S.; Hirosawa, K.; Kimura, M.; Hishida, A. & Ikegaya, N. Renal tubulointerstitial injury in weanling rats with hyperhomocysteinemia. *Kidney Int., 62(4)*:1219-28, 2002.

Li, A.; Liang, L.; Liang, P.; Hu, Y.; Xu, C.; Hu, X.; Shen, Y.; Hu, D.; Li, Z. & Kamel, I. R. Assessment of renal fibrosis in a rat model of unilateral ureteral obstruction with diffusion kurtosis imaging: Comparison with a-SMA expression and 18F-FDG PET. *Magn. Reson. Imaging, 66*:176-84, 2020.

Long, Y. & Nie, J. Homocysteine in renal injury. *Kidney Dis., 2(2)*:80-7, 2016.

Nee, L. E.; Mcmorrow, T.; Campbell, E.; Slattery, C. & Ryan, M. P. TNF-alpha and IL-1beta-mediated regulation of MMP-9 and TIMP-1 in renal proximal tubular cells. *Kidney Int., 66(4)*:1376-86, 2004.

Nishida, M.; Okumura, Y.; Ozawa, S.; Shiraishi, I.; Itoi, T. & Hamaoka, K. MMP-2 inhibition reduces renal macrophage infiltration with increased fibrosis in UUO. *Biochem. Biophys. Res. Commun., 354(1)*:133-9, 2007.

Ossani, G. P.; Fischer, P. A.; Caram, S. G.; Dominguez, G. N.; Monserrat, A. J. & Masnatta, L. D. Mild hyperhomocysteinemia promotes renal hemodynamic dysfunction without histopathologic changes in adult rats. *Kidney Int., 66(5)*:1866-72, 2004.

Sahraoui, A.; Dewachter, C.; de Medina, G.; Naeije, R.; Aouichat Bouguerra, S. & Dewachter, L. Myocardial structural and biological anomalies induced by high fat diet in *Psammomys obesus* gerbils. *PLoS One, 11(2)*:e0148117, 2016.

Saratlija Novakovic, Z.; Glavina Durdov, M.; Puljak, L.; Saraga, M.; Ljutic, D.; Filipovic, T.; Pastar, Z.; Bendic, A. & Vukojevic, K. The interstitial expression of alpha-smooth muscle actin in glomerulonephritis is associated with renal function. *Med. Sci. Monit., 18(4)*:CR235-40, 2012.

Sen, U.; Munjal, C.; Qipshidze, N.; Abe, O.; Gargoum, R. & Tyagi, S. C. Hydrogen sulfide regulates homocysteine-mediated glomerulosclerosis. *Am. J. Nephrol., 31(5)*:442-55, 2010.

Shishehbor, M. H.; Oliveira, L. P. J.; Lauer, M. S.; Sprecher, D. L.; Wolski, K.; Cho, L.; Hoogwerf, B. J. & Hazen, S. L. Emerging cardiovascular risk factors that account for a significant portion of attributable mortality risk in chronic kidney disease. *Am. J. Cardiol., 101(12)*:1741-6, 2008.

Tsai, J. P.; Liou, J. H.; Kao, W. T.; Wang, S. C.; Lian, J. D. & Chang, H. R. Increased expression of intranuclear matrix metalloproteinase 9 in atrophic renal tubules is associated with renal fibrosis. *PLoS One, 7(10)*:e48164, 2012.

Wang, Y. N.; Xia, H.; Song, Z. R.; Zhou, X. J. & Zhang, H. Plasma homocysteine as a potential marker of early renal function decline in IgA nephropathy. *Front. Med. (Lausanne), 9*:812552, 2022.

Yuan, D.; Chu, J.; Lin, H.; Zhu, G.; Qian, J.; Yu, Y.; Yao, T.; Ping, F.; Chen, F. & Liu, X. Mechanism of homocysteine-mediated endothelial injury and its consequences for atherosclerosis. *Front. Cardiovasc. Med., 9*:1109445, 2022.

Zhang, F.; Siow, Y. L. & O, K. Hyperhomocysteinemia activates NF-kB and inducible nitric oxide synthase in the kidney. *Kidney Int., 65(4)*:1327-38, 2004.

Corresponding author:
Billel Chaouad, Associate Professor
University of Khemis Miliana
Faculty of Natural and Life Sciences and Earth Sciences
Theniet El Had Road. 44225
Khemis Miliana
ALGERIA

ORCID ID: https://orcid.org/0000-0002-9223-2938

E- mail: b.chaouad@univ-dbkm.dz